SUPPLEMENTARY INFORMATION

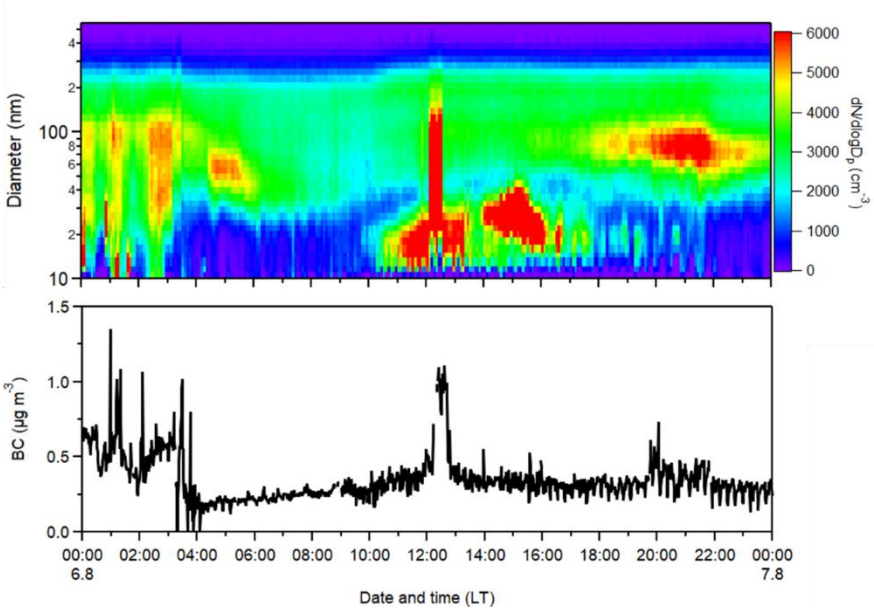

Figure S1: Example of a day where formation of new particles and subsequent growth is evident, but it is obstructed by emissions of nearby sources. The concentration of black carbon is also shown.

Table S1. Average meteorological conditions for each measurement site during the 2020 summer campaign.

Station	T (°C)	RH (%)	WS (m s^{-1})	SR (W m^{-2})
ATH	26±3.7	50±16	2±1.2	-
THES	25±3.3	68±11	2.3±2.1	-
PAT	26±3.8	55±18	3.0±1.9	259±322
IOA	23±6.0	63±25	1.0±0.9	243±327
THR	25±4.9	57±16	1.44±1.2	233±303
LES	-	-	-	-
SIF	27±2.4	55±11	2.8±1.6	-
FIN	25±2.2	70±14	6.8±2.6	259±322
CHA	26±3.5	64±14	6.9±5.3	
NEO	26±2.7	69±12	-	263±326
HAC	-	-	-	-

Table S2. Average meteorological conditions for each measurement site during the 2021 summer campaign.

Station	T (°C)	RH (%)	WS (m s^{-1})	SR (W m^{-2})
ATH	-	-	2.2±1.2	-
THES	-	-	-	-
PAT	27±3.9	51±15	2.9±1.7	287±345
IOA	25±6.6	53±25	1.1±1.0	271±343
THR	25±5.4	58±14	1.3±1.0	248±313
LES	25±4.2	59±14	3.8±3.2	-
SIF	28±3.5	56±14	2.76±1.5	304±366
FIN	26±3.3	65±15	8.4±2.6	291±331
CHA	27±4.3	60±15	7±5.4	253±297
NEO	-	-	-	-
HAC	13±5.1	66±25	3.4±1.2	-

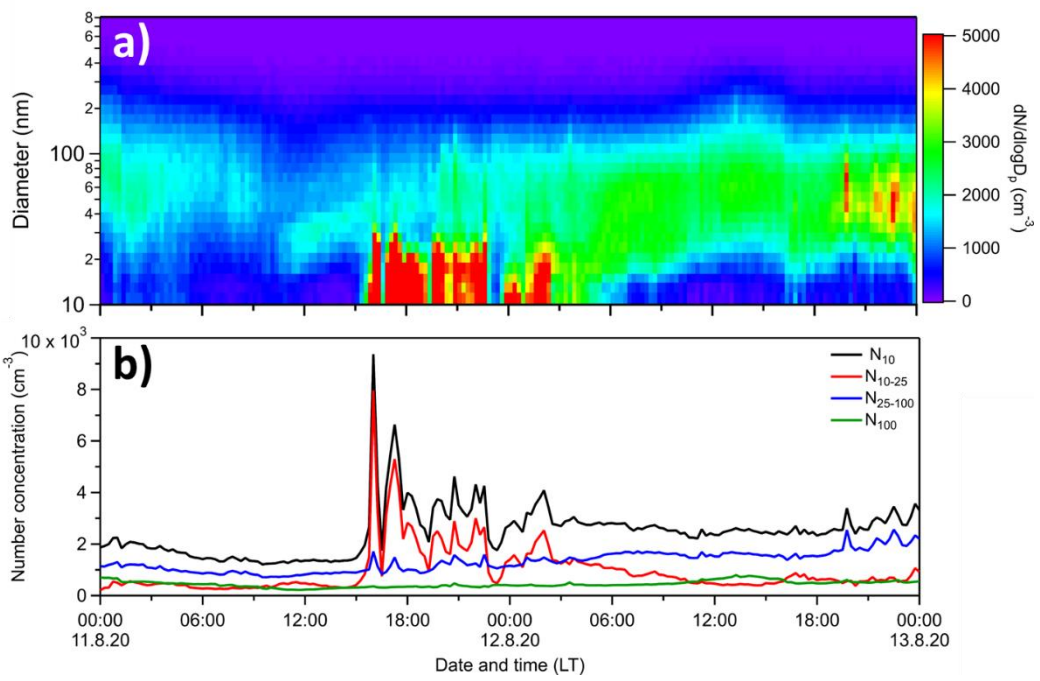

Figure S2: Example of a day where formation of new particles and subsequent growth is evident in NEO, but it is obstructed by emissions of nearby sources. The concentration of black carbon is also shown.

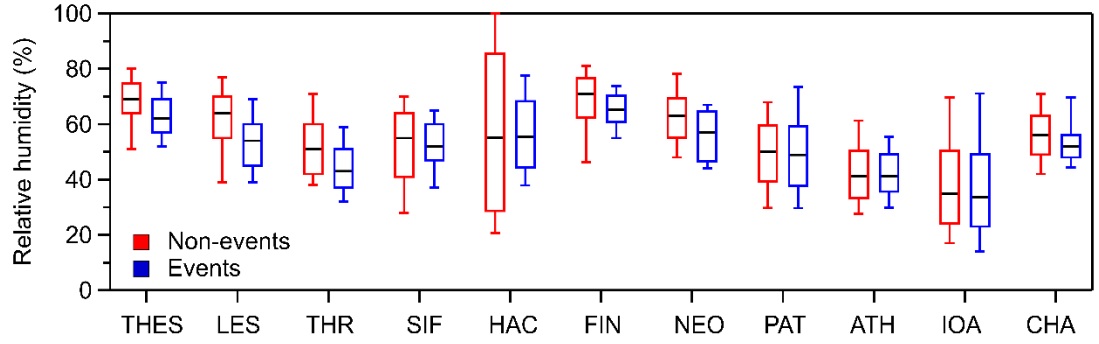

Figure S3: Comparison of the average relative humidity (RH) in the time period between 8:00 and 18:00 LT during nucleation events and non-events in each station. The black lines represent the median, while the box edges the 25th and 75th percentiles. The whiskers correspond to the 10th and 90th percentiles.

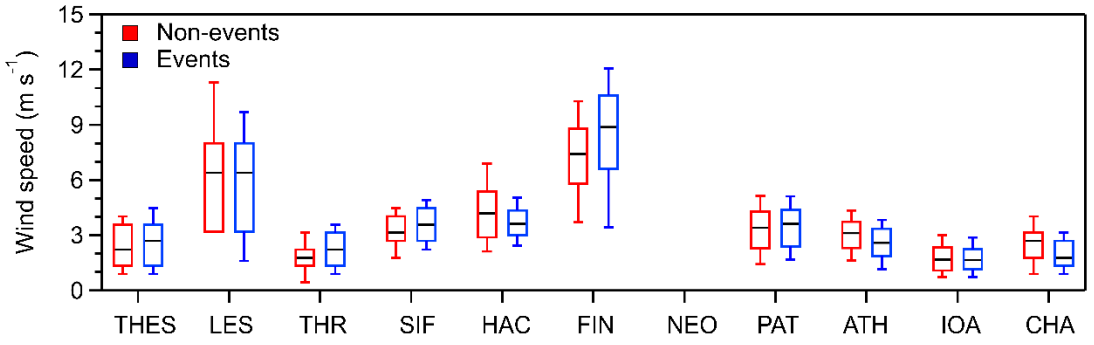

Figure S4: Comparison of the average wind speed in the time period between 8:00 and 18:00 LT during nucleation events and non-events in each station. The black lines represent the median, while the box edges the 25th and 75th percentiles. The whiskers correspond to the 10th and 90th percentiles.

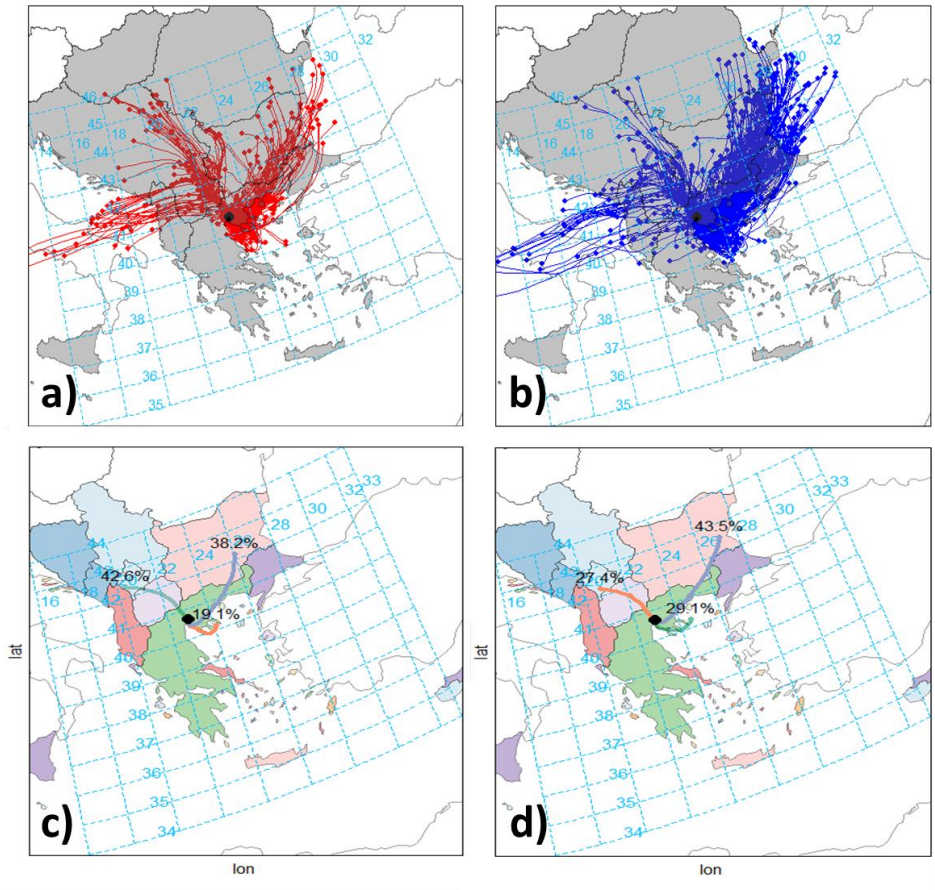

Figure S5: The 24-h backward air trajectories arriving at Thessaloniki during both campaigns in 2020 and 2021 for: a) NPF (Class I and II) events (257 trajectories); b) the whole period (877 trajectories). The probabilities of the air masses originating from a specific location during c) NPF events and d) the whole period is also shown. The trajectories shown for the NPF events correspond only to the hours during which the particles appeared during each event. The trajectories for the rest of the days correspond to the hours between 7:00–19:00 LT. Maps created by R version 4.1.1 using the Openair (Carslaw and Ropkins, 2012) version 2.16-0 and the MapData 2022 packages.

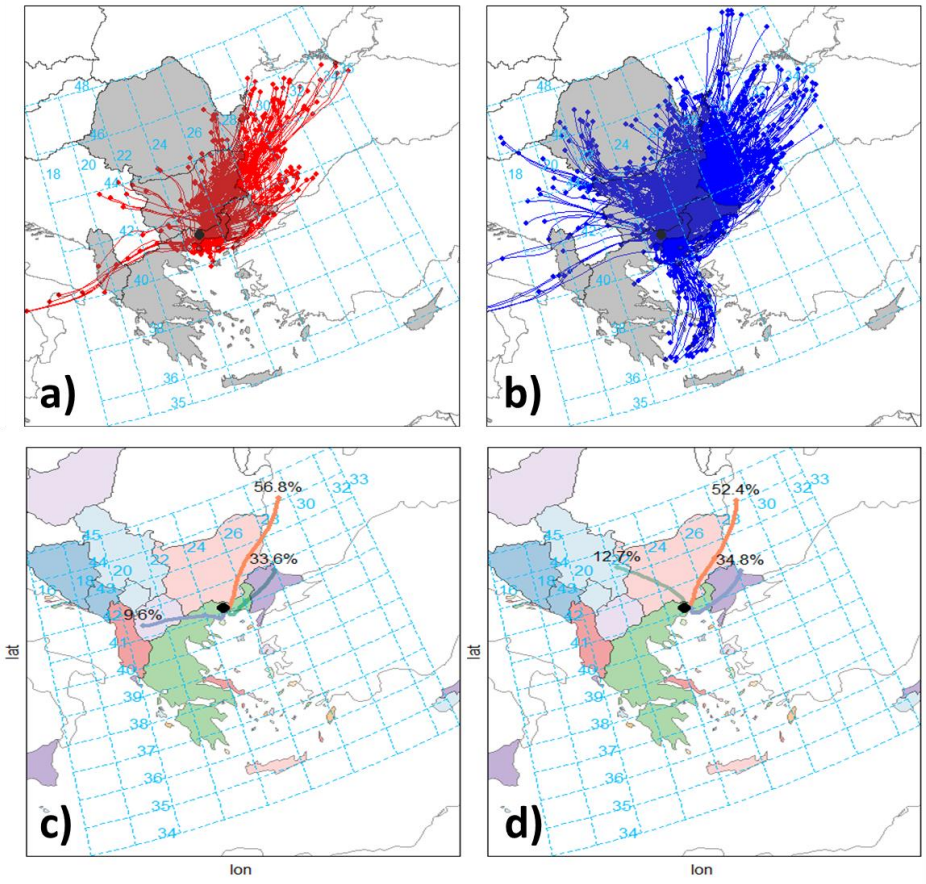

Figure S6: The 24-h backward air trajectories arriving at Thrace during both campaigns in 2020 and 2021 for: a) NPF (Class I and II) events (275 trajectories); b) the whole period (1227 trajectories). The probabilities of the air masses originating from a specific location during c) NPF events and d) the whole period is also shown. The trajectories shown for the NPF events correspond only to the hours during which the particles appeared during each event. The trajectories for the rest of the days correspond to the hours between 7:00–19:00 LT. Maps created by R version 4.1.1 using the Openair (Carslaw and Ropkins, 2012) version 2.16-0 and the MapData 2022 packages.

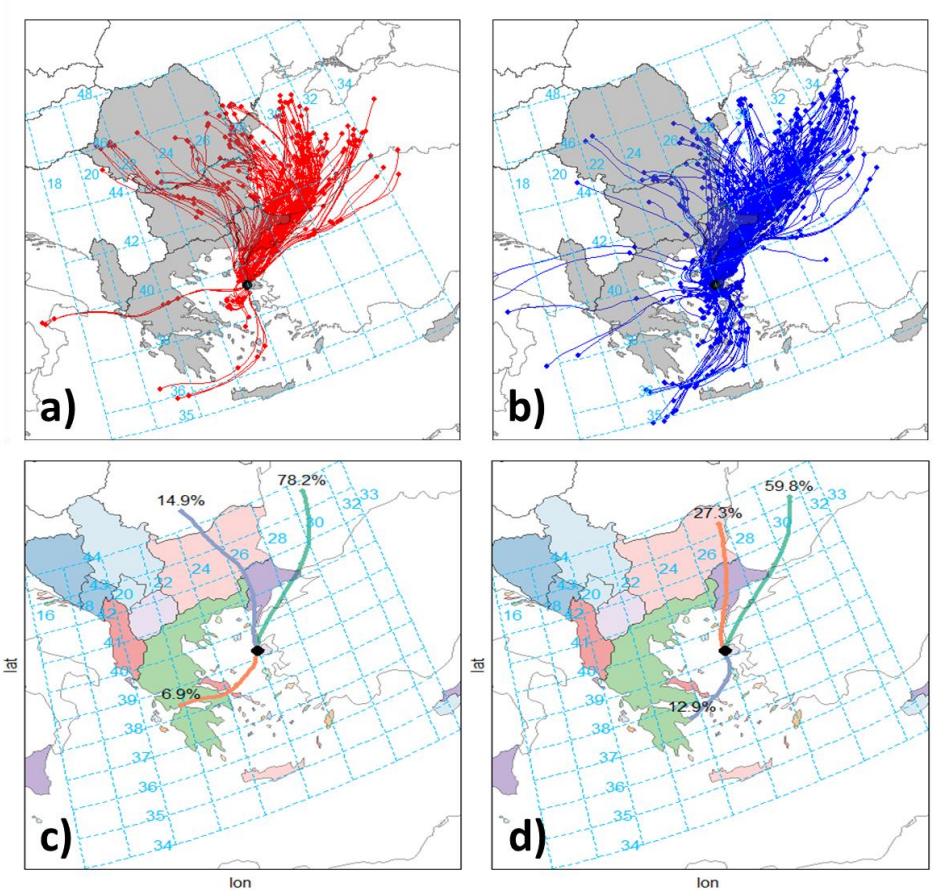

Figure S7: The 24-h backward air trajectories arriving at Lesvos during both campaigns in 2020 and 2021 for: a) NPF (Class I and II) events (197 trajectories); b) the whole period (543 trajectories). The probabilities of the air masses originating from a specific location during c) NPF events and d) the whole period is also shown. The trajectories shown for the NPF events correspond only to the hours during which the particles appeared during each event. The trajectories for the rest of the days correspond to the hours between 7:00–19:00 LT. Maps created by R version 4.1.1 using the Openair (Carslaw and Ropkins, 2012) version 2.16-0 and the MapData 2022 packages.

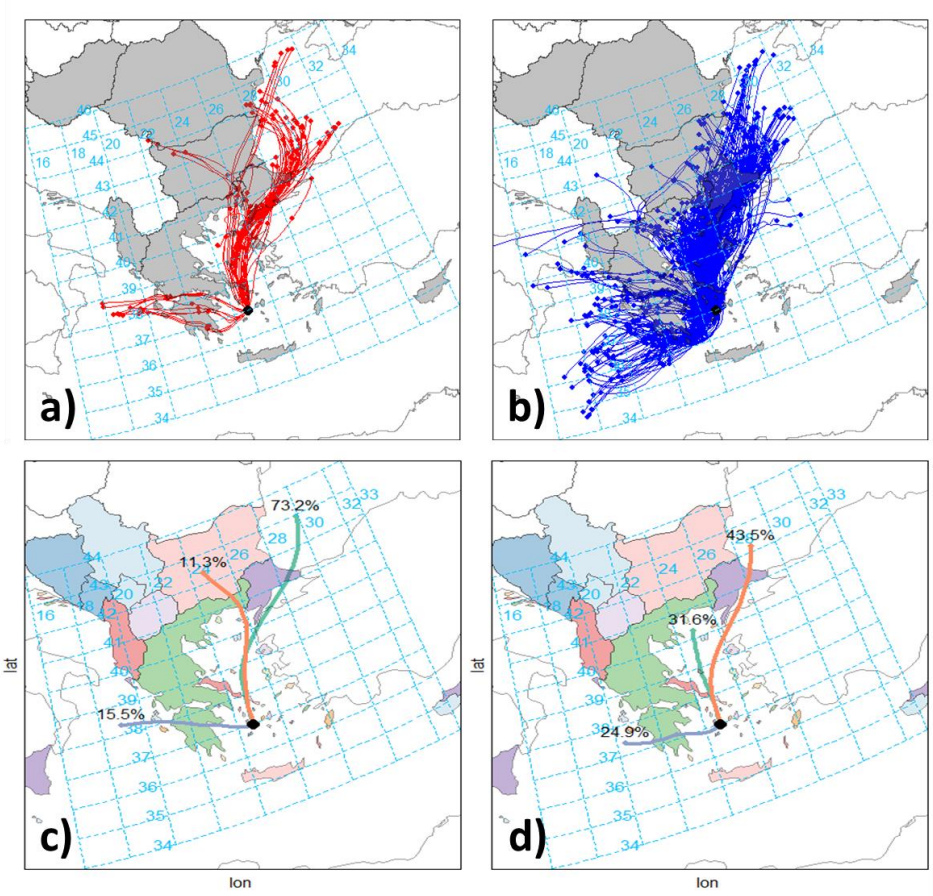

Figure S8: The 24-h backward air trajectories arriving at Sifnos during both campaigns in 2020 and 2021 for: a) NPF (Class I and II) events (134 trajectories); b) the whole period (880 trajectories). The probabilities of the air masses originating from a specific location during c) NPF events and d) the whole period is also shown. The trajectories shown for the NPF events correspond only to the hours during which the particles appeared during each event. The trajectories for the rest of the days correspond to the hours between 7:00–19:00 LT. Maps created by R version 4.1.1 using the Openair (Carslaw and Ropkins, 2012) version 2.16-0 and the MapData 2022 packages.

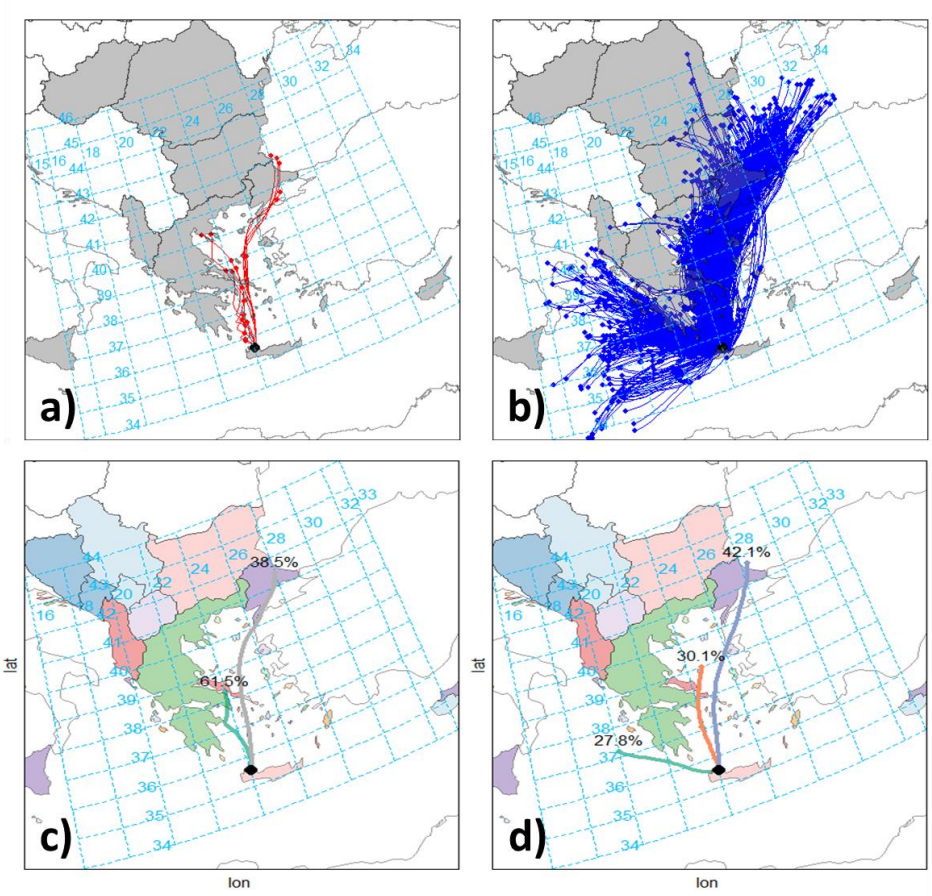

Figure S9: The 24-h backward air trajectories arriving at Chania during both campaigns in 2020 and 2021 for: a) NPF (Class I and II) events (13 trajectories); b) the whole period (1056 trajectories). The probabilities of the air masses originating from a specific location during c) NPF events and d) the whole period is also shown. The trajectories shown for the NPF events correspond only to the hours during which the particles appeared during each event. The trajectories for the rest of the days correspond to the hours between 7:00–19:00 LT. Maps created by R version 4.1.1 using the Openair (Carslaw and Ropkins, 2012) version 2.16-0 and the MapData 2022 packages.

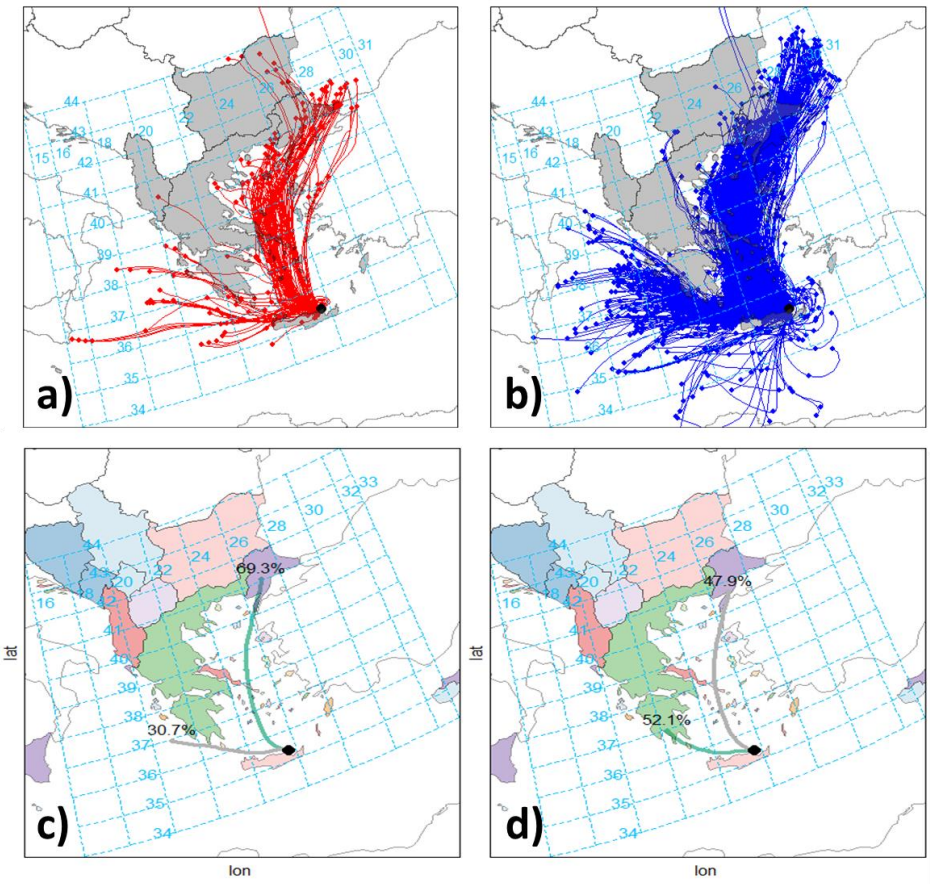

Figure S10: The 24-h backward air trajectories arriving at Finokalia during both campaigns in 2020 and 2021 for: a) NPF (Class I and II) events (178 trajectories); b) the whole period (1362 trajectories). The probabilities of the air masses originating from a specific location during c) NPF events and d) the whole period is also shown. The trajectories shown for the NPF events correspond only to the hours during which the particles appeared during each event. The trajectories for the rest of the days correspond to the hours between 7:00–19:00 LT. Maps created by R version 4.1.1 using the Openair (Carslaw and Ropkins, 2012) version 2.16-0 and the MapData 2022 packages.

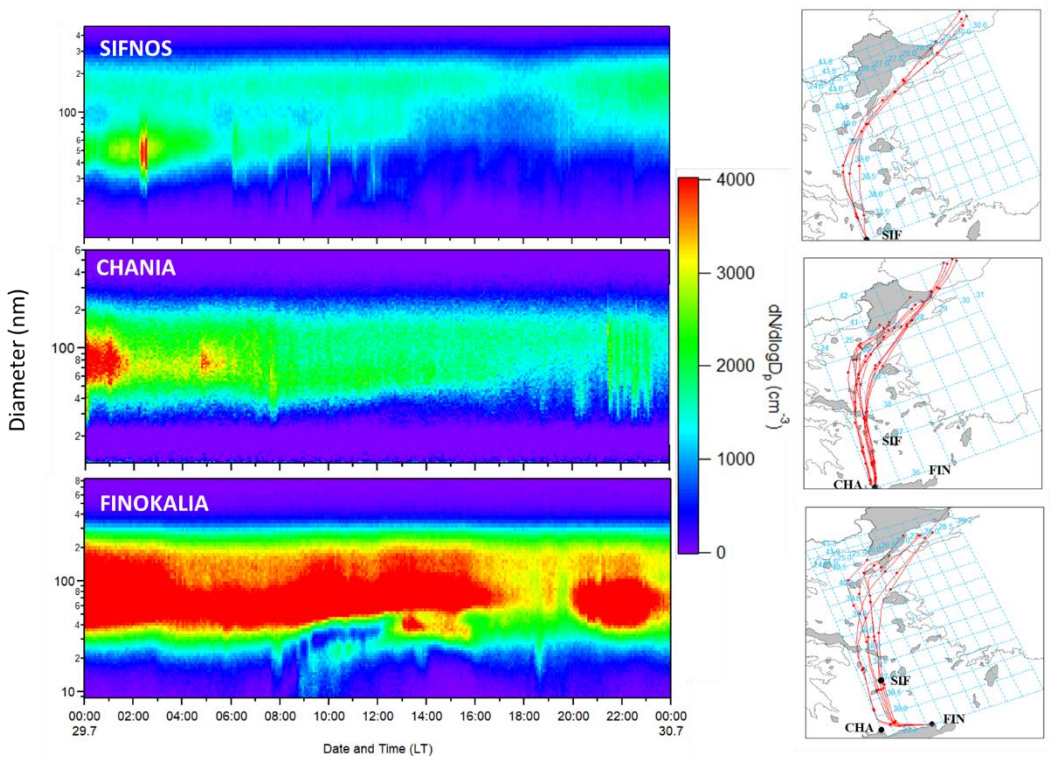

Figure S11: Particle number size distributions and the corresponding air mass trajectories (during the hours of the NPF event in Finokalia) in a) Sifnos, b) Chania and c) Finokalia. Maps created by R version 4.1.1 using the Openair (Carslaw and Ropkins, 2012) version 2.16-0 and the MapData 2022 packages.

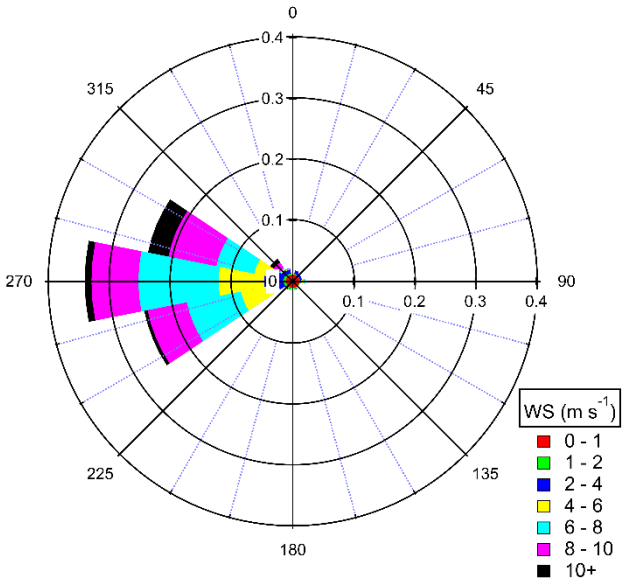

Figure S12: Local wind direction and speed during the summer campaign of 2020 in Finokalia.

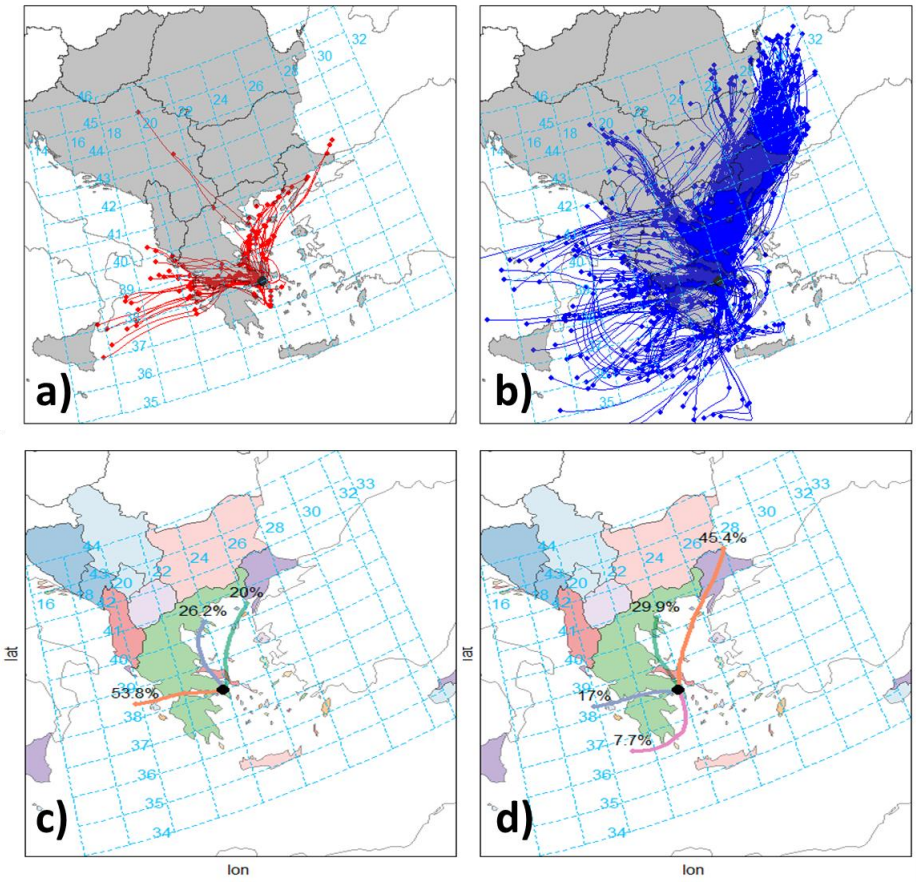

Figure S13: The 24-h backward air trajectories arriving at Athens during both campaigns in 2020 and 2021 for: a) NPF (Class I and II) events (73 trajectories); b) the whole period (1307 trajectories). The probabilities of the air masses originating from a specific location during c) NPF events and d) the whole period is also shown. The trajectories shown for the NPF events correspond only to the hours during which the particles appeared during each event. The trajectories for the rest of the days correspond to the hours between 7:00–19:00 LT. Maps created by R version 4.1.1 using the Openair (Carslaw and Ropkins, 2012) version 2.16-0 and the MapData 2022 packages.

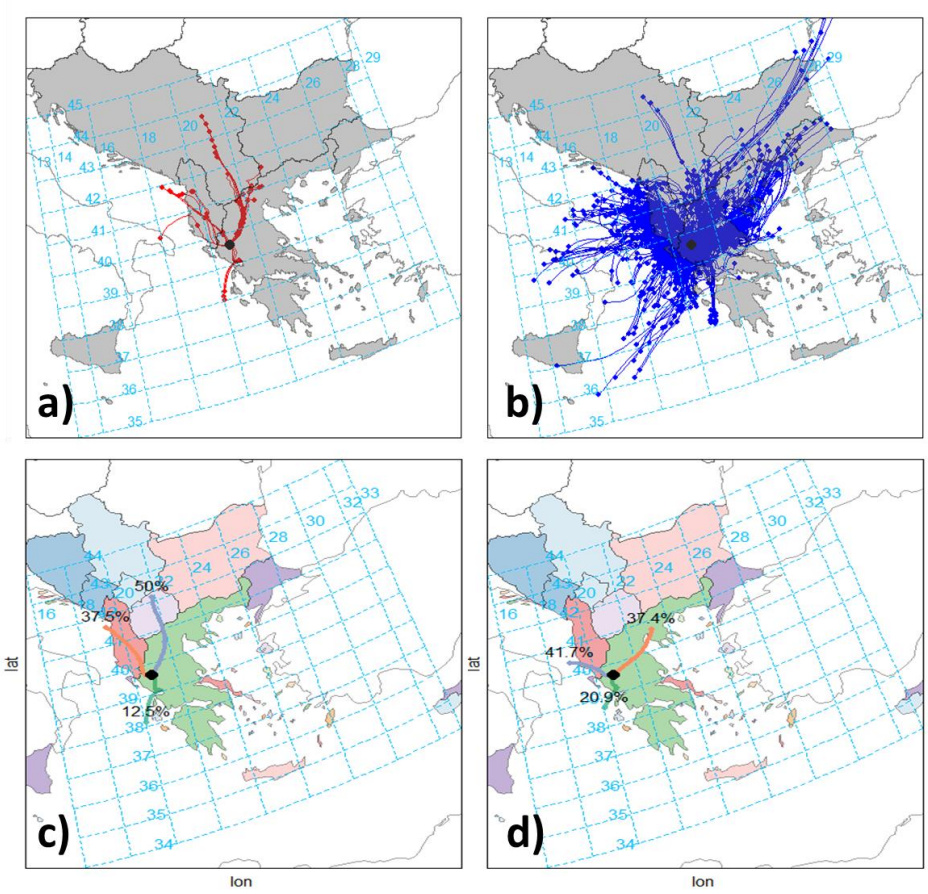

Figure S14: The 24-h backward air trajectories arriving at Ioannina during both campaigns in 2020 and 2021 for: a) NPF (Class I and II) events (26 trajectories); b) the whole period (809 trajectories). The probabilities of the air masses originating from a specific location during c) NPF events and d) the whole period is also shown. The trajectories shown for the NPF events correspond only to the hours during which the particles appeared during each event. The trajectories for the rest of the days correspond to the hours between 7:00–19:00 LT. Maps created by R version 4.1.1 using the Openair (Carslaw and Ropkins, 2012) version 2.16-0 and the MapData 2022 packages.